Cannabinoid inhibits HIV-1 Tat-stimulated adhesion of human monocyte-like cells to extracellular matrix proteins

Erinn S. Raborn, **Melissa Jamerson**, **Francine Marciano-Cabral**, and **Guy A. Cabral**
Department of Microbiology and Immunology, Virginia Commonwealth University, School of Medicine, Richmond, VA 23298

Abstract

Aims—The aim of this study was to assess the effect of select cannabinoids on human immunodeficiency virus type 1 (HIV-1) transactivating (Tat) protein-enhanced monocyte-like cell adhesion to proteins of the extracellular matrix (ECM).

Main Methods—Collagen IV, laminin, or an ECM gel were used to construct extracellular matrix layers. Human U937 monocyte-like cells were exposed to Tat in the presence of Δ^9-tetrahydrocannabinol (THC), CP55,940, and other select cannabinoids. Cell attachment to ECM proteins was assessed using an adhesion assay.

Key findings—THC and CP55,940 inhibited Tat-enhanced attachment of U937 cells to ECM proteins in a mode that was linked to the cannabinoid receptor type 2 (CB2R). The cannabinoid treatment of Tat-activated U937 cells was associated with altered β_1-integrin expression and distribution of polymerized actin, suggesting a modality by which these cannabinoids inhibited adhesion to the ECM.

Significance—The blood-brain barrier (BBB) is a complex structure that is composed of cellular elements and an extracellular matrix (ECM). HIV-1 Tat promotes transmigration of monocytes across this barrier, a process that includes interaction with ECM proteins. The results indicate that cannabinoids that activate the CB2R inhibit the ECM adhesion process. Thus, this receptor has potential to serve as a therapeutic agent for ablating neuroinflammation associated with HIV-elicited influx of monocytes across the BBB.

Keywords

cannabinoid; cell adhesion; extracellular matrix; HIV; monocyte-like cells; Tat; U937 cells

Corresponding Author: Guy A. Cabral, Ph.D., Department of Microbiology and Immunology, Virginia Commonwealth University, School of Medicine, 1101 E. Marshall Street, Richmond, VA 23298-0678, Tel: 804-828-2306, Fax: 804-828-9946, gacabral@vcu.edu.

Introduction

The blood-brain barrier (BBB) separates circulating blood from the central nervous system (CNS) extracellular fluid that occurs along capillaries reviewed in (Rubin and Staddon 1999). It is comprised of an endothelial cell layer that restricts the diffusion of molecules and plays an active role in the transport of metabolic products, astrocytic endfeet, and a thick basement membrane that harbors several large glycoproteins that form an organized matrix. This extracellular matrix (ECM) provides structural support to tissue and serves as a cue for activation of cell proliferation, differentiation, and migration (Lukashev and Werb 1998; Mareel and Leroy 2003; Larsen et al. 2006; Berrier and Yamada 2007).

The Human Immunodeficiency Virus-1 (HIV-1) invades the CNS, presumably through the migration of virally-infected leukocytes across the BBB (Buckner et al. 2006). Infected leukocytes are carriers of virus and secrete chemokines, cytokines, and viral-specified gene products such as the regulatory trans-activating protein (Tat) and the envelope glycoprotein 120 (gp120) (Schneider et al. 1986; Ensoli et al. 1993; Zink et al. 1999). The combined action of these extracellular factors engenders an inflammatory cascade from bystander immunocytes that compromises the integrity of the BBB. This inflammatory response, characterized by cell infiltration and microglial cell activation, may correlate more strongly with the degree of neurological impairment than does HIV-1 load in the CNS (Glass et al. 1993).

The Tat protein is essential for efficient replication of the HIV (Laspia et al. 1989; Ensoli et al. 1993). It interacts with cell surface receptors related to cell adhesion and motility, including chemokine receptors and cell adhesion molecules (Lafrenie et al. 1996). It also can modulate the expression of cellular genes related to survival, growth, inflammation, and angiogenesis (Chang et al. 1995), induce the production of cytokines (Pu et al. 2003) and chemokines (D'Aversa et al. 2004), and increase the migration and invasion of various cell types such as monocytes, basophils, mast cells, microglia, and endothelial cells (Lafrenie et al. 1996; de Paulis et al. 2000; Avraham et al. 2004; Eugenin et al. 2005).

Cannabinoids have been reported to alter the functional activities of a variety of immune cells, including their ability to migrate in response to inflammatory stimuli and virus-specified gene products (reviewed in Cabral and Staab 2005; Raborn and Cabral 2010; Kong et al. 2014). A select number of these affected activities has been reported to be consequent of activation of G inhibitory (G_i) protein-coupled seven-transmembranal cannabinoid receptors (reviewed in Cabral and Staab 2005). To date, two receptors that meet stringent pharmacological and molecular criteria for designation as cannabinoid receptors have been identified. The cannabinoid receptor type 1 (CB1R) has been localized primarily to the CNS and testis while the cannabinoid receptor type 2 (CB2R) has been localized primarily to cells of the immune system. In the present study, we demonstrate that the cannabinoids Δ^9-tetrahydrocannabinol (THC) and CP55,940 inhibit Tat-promoted adhesion of human U937 monocyte-like cells to proteins that are found in the ECM. Furthermore, this inhibition was found to be linked to the CB2R. In addition, we observed altered expression of β_1-integrin and redistribution of polymerized actin, suggesting a mode by which these cannabinoids inhibited adhesion of macrophage-like cells to the ECM. Since the ECM is a critical

component of the BBB, the results suggest that the CB2R has potential to serve as a molecular target for therapeutic ablation of Tat-stimulated transmigration of monocytes into the CNS.

Materials and methods

Cell culture

The human leukemic monocyte lymphoma cell line U937 was obtained from the American Type Culture Collection (ATCC CRL-1593.2). Cells were cultured in RPMI 1640 medium (Cellgro, Herndon, VA) containing 10% fetal bovine serum supplemented with 1% L-glutamine, 1% nonessential amino acids, 1% MEM vitamins, 0.01M HEPES and penicillin [100 U/ml]/streptomycin [100 μg/ml]/fungizone [0.25 μg/ml](Cellgro).

Cannabinoids

The partial agonist at the cannabinoid receptor types 1 and 2 (i.e., CB1R/CB2R) THC (Δ^9-tetrahydrocannabinol, (6aR,10aR)-6,6,9-trimethyl-3-pentyl-6a,7,8,10a-tetrahydro-6H-benzo[c]chromen-1-ol), the CB2R- selective ligand O-2137 ((1R,3R)-1-[4-(1,1-dimethylheptyl)-2,6-dimethoxyphenyl]-3-methylcyclohexanol), the CB1R antagonist SR141716A (5-(4-chlorophenyl)-1-(2,4-dichlorophenyl)-4-methyl-N-(piperidin-1-yl)-1H-pyrazole-3-carboxamide) and the CB2R antagonist SR144528 (5-(4-chloro-3-methylphenyl)-1-[(4-,methylphenyl)methyl]-N-[1R,3S,4S)-2,2,4-trimethyl-3-biccyclo[2.2.1]heptanyl]pyrazole-3-carboxamide) were obtained from the Department of Pharmacology and Toxicology (Virginia Commonwealth University, Richmond, VA). 2-AG (2-Arachidonoylglycerol, 1,3-dihydroxypropan-2-yl (5Z,8Z,11Z,14Z)-icosa-5,8,11,14-tetraenoate), the CB1R-selective agonist ACEA (Arachidonyl-2-chloroethylamide, N-(2-Chloroethyl)-5Z,8Z,11Z,14Z-eicosatetraenamide), the full CB1R/CB2R agonist CP55,940 (2-[(1R,2R,5R)-5-hydroxy-2-(3-hydroxypropyl) cyclohexyl]-5-(2-methyloctan-2-yl)phenol), and abnormal cannabidiol (abn-cbd, 4-[(1S,6R)-3-methyl-6-prop-1-en-2-ylcyclohex-2-en-1-yl]-5-pentylbenzene-1,3-diol) were purchased from Tocris Bioscience, R&D Systems (Minneapolis, MN). Stock solutions of cannabinoids (10^{-2} M) were prepared in 100% ethanol and stored at −20°C. Ethanol (0.01%) in medium was used as the cannabinoid vehicle control.

Tat

Recombinant human HIV-1 Tat$_{1-86}$ protein was obtained from Immunodiagnostics, Inc. (Woburn, MA), dissolved in sterile Phosphate-buffered Saline (PBS) to obtain a stock solution (10 μM) and frozen in aliquots at −80°C until converted to a working solution according to the manufacturer's recommendation. For *in vitro* administration, low-retention microfuge tubes (Fisher, Pittsburgh, PA) and low-binding pipette tips (VWR, Suwanee, GA) were used to minimize Tat loss due to tube or pipette surface adsorption.

Extracellular matrix coating

Ninety-six well plates were incubated (10 μg/ml) overnight at 4°C with collagen IV (Coll IV) or laminin (LM) derived from Engelbreth-Holm-Swarm murine sarcoma basement membrane (Sigma-Aldrich, St. Louis, MO; Invitrogen, Grand Island, NY). Prior to use,

unpolymerized Coll IV or LM was removed and the wells were washed once with PBS. Alternately, wells were coated with ECM gel (Sigma-Aldrich, St. Louis, MO) that forms a reconstituted basement membrane consisting of laminin, type IV collagen, heparan sulfate proteoglycan, entactin, and other minor components. ECM gel (stock solution 8 mg/ml) was diluted 1:3 in RPMI 1640 medium without serum and added to wells for 10 min at room temperature. Following removal of excess unpolymerized ECM gel, the plates were incubated (2h, 37°C) for drying prior to use.

Adhesion assay

Cells were treated (2h, 37°C) in RPMI 1640 medium without serum containing PBS or Tat (10–50nM) in the presence of vehicle (0.01% ethanol) or cannabinoid (1 μM). Following treatment, cells (4×10^4) were added to Coll IV, LM, or ECM gel-coated wells for 30 min at 37°C. Wells then were washed 3 times with PBS to remove unbound cells and bound cells were fixed with 2% glutaraldehyde in 0.1M cacodylate buffer, pH 7.2. Three random video still images/well of triplicate wells were captured using an Olympus CK2 inverted microscope (Opelco, Washington, DC) equipped with an attached XV-GP230 digital video camera (Panasonic, Yokohama, Japan) interfaced to a Dell Dimension XPS1450 computer using Videum 100 hardware and Window NT software (Winnov, Sunnyvale, CA). Each experiment was performed three times in triplicate. The average of the sum of 3 image fields from 3 wells of a given experimental group was represented graphically on the ordinate-axis as "cells".

Invasion assay

Transwell tissue culture inserts (8 μm pore size, Corning Costar) pre-loaded into 24-well tissue culture plates were coated (100 μl, 10 min) with ECM gel (2.7 mg/ml; Sigma-Aldrich). Unpolymerized solution was removed following the coating period (10 min), and the inserts were allowed to dry (2h, 37°C). Serum-free RPMI 1640 medium was added to the bottom well of the transwell apparatus. Cells (10^6/100 μl) were treated (24h, 37°C) in RPMI 1640 medium without serum containing PBS or Tat (50nM) in the presence of vehicle (0.01% ethanol) or cannabinoid (1 μM) and added to the insert and the transwell apparatus was incubated for 24h (at 37°C). Cells that passed through the ECM-coated inserts and into the bottom well were counted by capturing five random video still images/well as described above. Experiments were performed twice in quadruplicate. The average of the sum of 5 image fields from 4 wells of a given experimental group was represented graphically on the ordinate-axis as "cells".

Real-time reverse transcriptase polymerase chain reaction

Total RNA from U937 cells was prepared using TRIzol reagent (Invitrogen) according to the manufacturer's instructions. RNA was isolated using phenol/chloroform extraction and was resuspended in PCR-grade water. The isolated RNA was purified for removal of residual genomic DNA using an RNeasy Mini Kit (Qiagen, Valencia, CA). Reverse transcription to generate complementary DNA (cDNA) was performed using the SuperScript III First Strand Synthesis System (Invitrogen) with random hexamer primers. SYBR green real-time PCR was performed using the RT^2 PCR primer sets for the human CB1R (NCBI accession NM_016083.3), human CB2R (NCBI accession NM_001841.1),

GPR55 (NCBI accession NM_005683.3) and glyceraldehyde 3-phosphate dehydrogenase (GAPDH; NCBI accession NM_002046.3)(Qiagen). Each 25 μl PCR reaction contained 12.5 μl 2× RT^2 Real-time SYBR Green PCR Master Mix (Qiagen), 2 μl sample cDNA, 1 μl RT^2 PCR Primer set, and PCR grade water. Amplification was performed using the following program: 95°C, 15 min and 40 cycles of 95°C, 30 sec; 55°C, 30s; and 72°C, 30s. PCR amplicons (CB2R: 185 bp, GPR55: 137 bp, GAPDH: 175 bp) were visualized by agarose gel electrophoresis (100V) using OmniPure Agarose PCR plus gel (4%)(VWR) in 1× Tris/borate/EDTA buffer.

SDS-polyacrylamide gel electrophoresis and western immunoblotting

U937 cells were treated with Tat in the presence or absence of cannabinoid (1 μM: THC, CP55,940; 2h at 37°C), then collected and centrifuged (3000 × g, 10 min, 4°C). Cell pellets were resuspended in cell lysis buffer containing deionized water and protease inhibitor cocktail (100:1; 4-(2-aminoethyl) benzenesulfonyl fluoride, pepstatin A, E-64, bestatin, leupeptin, and aprotinin; Sigma-Aldrich). The whole cell lysates were subjected to three freeze-thaw cycles of liquid nitrogen for 1 min, followed by insertion into a 37°C water bath for 2 min and thorough mixing. Protein concentration was determined using the Bradford assay (Bradford 1976). Whole cell lysates (30 μg) were prepared in reducing sample buffer containing SDS and β-mercaptoethanol, heated at 95°C (10 min), and separated by 10% SDS-PAGE. Proteins were transferred to a Transblot nitrocellulose membrane (BioRad Laboratories, Hercules, CA), which was probed with anti-human CB2R primary antibody (1:100)(Nowell et al. 1998) or anti-human GPR55 primary antibody (5 μg/ml) (Cayman Chemical) overnight at 4°C followed by goat anti-rabbit IgG-HRP conjugated secondary antibody (1:2000, CB2R; 1:5000, GPR55) at room temperature for 2h. Proteins were detected using enhanced chemiluminescence (ECL Prime Western Blotting Reagents, GE Healthcare, Little Chalfont, Buckinghamshire, UK) with exposure on Kodak BioMax XAR film (Eastman Kodak, Rochester, NY). The nitrocellulose membranes were stripped and re-probed with an anti-actin antibody (1:1000, MP Biomedicals, Solon, OH) to verify equivalent loading of samples. Densitometric analysis was accomplished using a ScanMaker 9800XL scanner (Microtek Lab Inc., Santa Fe Springs, CA) in concert with Quantity One 1-D Analysis software (Bio-Rad Laboratories, Inc., Hercules, CA).

Scanning electron microscopy

Cells adhered to ECM substrates layered on glass coverslips were subjected to fixation by immersion in 2% glutaraldehyde in 0.1M cacodylate buffer, pH 7.2. Coverslips then were washed four times with PBS, and treated (40 min in the dark) with 2% (w/v) osmium tetroxide buffered in 0.1 M cacodylate buffer, pH 7.2. Following a wash with PBS, coverslips were subjected to dehydration in a graded series of ethanol solutions, subjected to critical-point drying with CO_2 as the transitional fluid, mounted on stubs and coated with gold (30 nm). Samples were examined in a Zeiss EVO 50XVP scanning electron microscope operating at an accelerating voltage of 15 kV.

Confocal Microscopy

U937 cells (6×10^4) were pretreated with Tat in the presence or absence of cannabinoid (1 μM; THC, CP55940; 2h at 37°C), then seeded in Lab-Tek Chamber Slides (Nunc,

ThermoFisher Scientific, Waltham, MA) precoated with Coll IV (20 μg/ml) and incubated at 37°C (1h) to allow for cellular adhesion. The cells were fixed in 4% paraformaldehyde (1h) and rinsed in PBS. Cells were permeabilized with 0.1% Triton X-100 in PBS (20 min) then blocked with 5% BSA in PBS (1h). Immunofluorescent staining was performed using a FITC-conjugated anti-human β_1- integrin antibody (1:250, 2h)(Millipore, Billerica, MA), followed by AlexaFluor594-conjugated Phalloidin to visualize F-actin (1:500, 2h) (Invitrogen). Cells were counterstained with DAPI (1:20,000, 5 min)(Invitrogen) for nuclear identification. ProLong Gold Antifade Reagent (Invitrogen) was used for mounting of the coverslips in addition to stabilization of the immunofluorescent signal. Image acquisition was performed using a BX51 microscope with a spinning disk unit (Olympus, Center Valley, PA) and an Orca-R2 CCD camera (Hamamatsu, Japan). Images then were processed using the Slidebook software package (Intelligent Imaging Innovations, Denver, CO, USA).

Statistics

One Way Analysis of Variance (ANOVA) was performed to assess for differences between treatment groups. Control groups and cannabinoid treatment groups were compared with the maximal response elicited by the group treated with Tat +0.01% ethanol. Bonferroni's t-test was used to compare differences in Tat-treated cells versus cells treated with cannabinoid in the presence of Tat, in addition to differences between treatment groups.

Results

Cannabinoid receptor profile of U937 human monocyte-like cells

SYBR green RT-PCR was used to assess the cannabinoid receptor mRNA profile of U937 cells. Messenger RNA for the CB1R was not detected. However, mRNA for the CB2R and GPR55 was present, as demonstrated by the 185 and 137 bp amplification products obtained from untreated U937 total whole cell RNA (Fig. 1A). Western immunoblot analysis confirmed the expression of the CB2R and GPR55 (Fig. 1B) at the protein level. Additionally, U937 cells were exposed *in vitro* to Tat (50 nM) or to Tat in the presence of 1μM THC or CP55,940 and the relative levels of CB2R and GPR55 protein were determined. Drug vehicle (0.01% ethanol) or Tat ± cannabinoid had no major observable effect on protein levels of the CB2R or GPR55 (Fig. 1B).

Tat increases adhesion of human U937 monocyte-like cells to proteins of the ECM

Initial experiments were performed to confirm that U937 cells adhered to proteins of the ECM and to determine whether this adhesion was differential in relation to Coll IV, LM, or ECM gel. Cells exhibited minimal adhesion to uncoated wells in the presence or absence of Tat and minimal adhesion to the three ECM substrates in the absence of Tat (Fig. 2). Treatment of cells with Tat resulted in a concentration-related increase in adhesion to Coll IV, LM, and ECM gel. Optimal adhesion to Coll IV, LM, and ECM gel was obtained when cells were treated with 50 nM Tat. At this concentration of Tat, adhesion of cells to Coll IV or LM superseded that obtained for ECM gel. Ethanol at 0.01% concentration in medium had no observable effect on adhesion of U937 cells to Coll IV, LM, or ECM gel (Data not shown).

The cannabinoid CP55,940 inhibits adhesion of U937 cells to proteins of the ECM

Cells were maintained in medium containing vehicle, CP55,940 (1 μM), Tat, or Tat in the presence of CP55,940 (1 nM–1μM). Minimal levels of adhesion to any of the ECM substrates were observed when cells were treated with vehicle or CP55,940 alone. Cells treated with Tat exhibited a relatively high level of adhesion to Coll IV (Fig. 3A), LM (Fig. 3B), or ECM gel (Fig. 3C). CP55,940 treatment significantly inhibited in a dose-related fashion Tat-enhanced adhesion to Coll IV. A similar, but less robust, outcome was obtained when LM and ECM were used as substrates. Scanning electron microscopy was performed in tandem with these adhesion assessments in order to gain insight regarding U937 cell conformational interaction with Coll IV. Figures 3D–G are illustrative of this interaction. Vehicle-treated cells exhibited a rounded morphology (Fig. 3D), but consistent with the adhesion experiments, a low number of adherent cells was observed (Data not shown). Cells treated with Tat plus vehicle exhibited a flattened appearance and displayed numerous cellular projections (Fig. 3E). In contrast, cells treated with THC plus Tat (Fig. 3F) or CP55,940 plus Tat (Fig. 3G) were rounded in appearance and exhibited a reduced number of cellular projections. Cells treated only with CP55,940 appeared morphologically similar to those treated with vehicle in the absence of Tat (Data not shown).

The experiments indicative of a CP55,940-mediated inhibition of Tat-promoted adhesion to ECM proteins were performed on a two-dimensional substratum matrix. Thus, in order to confirm that such a substratum did not serve as a physical barrier to passage of U937 cells, invasion experiments were performed. ECM gel was used in the three-dimensional matrix construct since it included Coll IV and LM and represented the most complex substratum composite used in this study (Fig. 4). U937 cells treated with vehicle exhibited a minimal level of passage through the matrix into the bottom well while U937 cells treated with Tat exhibited a three-fold increase in the level of migration into the bottom well.

Exposure of cells to Tat in concert with THC or CP55,940 (1 μM) resulted in the inhibition of their migration into the bottom well. The level of THC or CP55,940-mediated inhibition of "invasion" approximated that which was recorded for vehicle-treated cells.

Pharmacological linkage of cannabinoid-mediated inhibition of cell adhesion to the CB2R

To garner insight as to the range of cannabinoids that inhibited Tat-enhanced adhesion to ECM proteins, U937 cells were treated with THC, CP55,940, ACEA, O-2137, 2-AG, or Abn-CBD in the presence or absence of Tat (50 nM) (Fig. 5). Minimal levels of adhesion were observed when cells were treated with medium containing vehicle or cannabinoid alone. Cells treated with Tat exhibited a maximal level of adhesion to Coll IV (Fig. 5A), LM (Fig. 5B), or ECM gel (Fig. 5C). In contrast, U937 Tat-enhanced cell adhesion to each substrate was inhibited (30–50%) by THC (a partial CB1R/CB2R agonist), CP55,940 (a full agonist at the CB1R and CB2R), O-2137 (a CB2R-selective ligand), 2-AG (a CB1R/CB2R endocannabinoid agonist), or Abn-CBD (a candidate GPR55 agonist). Tat-enhanced adhesion to Coll IV, LM, or ECM gel was not affected when cells were treated with the CB1R-selective agonist ACEA.

In order to extend these pharmacological results, the CB1R-selective antagonist SR141716A (SR1) and the CB2R-selective antagonist SR144528 (SR2) were used in experiments. Cells were pre-treated (1 μM, 30 min) with either antagonist prior to exposure to medium containing Tat and CP55,940 (1 μM, 2h). Neither antagonist in itself affected adhesion of U937 cells to any of the matrix substrates (Fig. 6). As expected, CP55,940 inhibited Tat-enhanced adhesion of U937 cells. In contrast, while SR1 had no effect on the CP55,940-mediated reduction of Tat-enhanced adhesion to ECM proteins, treatment with SR2 resulted in reversal of CP55,940-mediated inhibition of adhesion, consistent with a pharmacological linkage to the CB2R (Figs. 6A–C).

Cannabinoid Treatment Alters Pattern of β_1-integrin and Actin Distribution

Since β_1-integrin and F-actin are critical proteins involved in cell adhesion and motility, confocal microscopy was performed to assess the effects of THC or CP55,940 on their distribution in U937 cells in the context of Tat exposure (Fig. 7). Cells treated with Tat (2h) and cultured on a Coll IV substratum (1h) exhibited an apparent increased level of expression of β_1-integrin relative to vehicle-treated cells. Staining for F-actin was prominent at cytoplasmic projections from U937 cells. In addition, immunostaining for β_1 integrin appeared to be co-localized with F-actin and at the outer edges of the cell membrane (Fig. 7, first column, row four). In contrast, U937 cells treated (1 μM, 2h) with THC or CP55,940 in the presence of Tat (50 nM) exhibited a rounded appearance, an uniform cytoplasmic distribution of staining for F-actin, and an altered distribution as well as an apparent reduction in the overall level of β_1-integrin(Fig. 7, first column, row five and six, respectively). Furthermore, these cells exhibited a small punctate pattern of β_1 integrin distribution (Fig. 7, second column, row five and six, respectively).

Discussion

The Tat protein is an early HIV-specified RNA-binding protein that plays a crucial role in HIV replication (Arya et al. 1985; Dayton et al. 1986). At initiation of infection, large amounts of Tat are synthesized and released that then can translocate across cell membranes, localize in the nucleus of other infected cells, and drive virus replication (Ensoli et al. 1993; Watson and Edwards 1999). In addition, Tat contains a chemokine-like domain (Cys-Cys-Phe sequence) characteristic of many β-chemokines (Albini et al. 1998), which allows for its interaction with chemokine receptors on the surface of immune cells. Thus, Tat also promotes migration of microglia (Eugenin et al. 2005; Fraga and Raborn et al. 2011) and monocytes (Albini et al. 1998) and induces Ca^{2+} fluxes through the chemokine receptors CCR2 and CCR3 (Albini et al. 1998). Indeed, cross-desensitization experiments have demonstrated that Tat displaces the β-chemokines MCP-1, MCP-3, and eotaxin (Albini et al. 1998). It has been demonstrated also that Tat binds to, and activates, the α-chemokine receptor CXCR4 (Ghezzi et al. 2000). Furthermore, it has been reported that Tat enhances monocyte adhesion by up-regulation of ICAM-1 and VCAM-1 gene expression (Dhawan et al. 1992; Song et al. 2007). Thus, Tat exerts a variety of effects on migration, adhesion molecule expression, and cell adhesion that promote monocyte invasion into the brain (Pu et al. 2003; Weiss et al. 1999).

The BBB is a highly dynamic structure, regulated by the interaction of cellular and ECM components that mediate the transport of cells and molecules into the CNS. Cellular components include endothelial cells that line cerebral blood vessels, astrocytes, pericytes, and microglia. ECM proteins include collagen IV and laminin, components that are critical in basement membrane assembly and that have direct effects on the physiological properties of the BBB (reviewed in Baeten and Akassoglou 2011). During the invasion of the CNS, activated monocytes interact with proteins of the ECM, an interaction that is integral to the process of leukocyte migration across endothelium (Muller and Randolph 1999). This observation, taken in the context that exposure to Tat promotes chemotaxis (Mitola et al. 1997; Albini et al. 1998) and enhances cell adhesion, suggests that interaction of monocytes with the ECM plays a critical role in their passage into the CNS.

Human U937 promonocytic cells (Sundstrom and Nilsson 1976) were used in the present study to analyze the effect of cannabinoids on Tat-enhanced adhesion to ECM proteins. These cells exhibit phenotypic and functional properties of human monocytes (Pucillo et al. 1993; Zella et al. 1998) and have been used extensively to model HIV-1 infection (Cassol et al. 2006) and HIV-1 latency (Emiliani et al. 1998) and to assess effects of HIV-1 infection on the activities of antigen-presenting cells (Zella et al. 1998). These cells also exhibit an up-regulation of cytokine expression following exposure to exogenously introduced Tat (Leghmari et al. 2008). Finally, the U937 cells express the CB2R and GPR55, but not the CB1R, a receptor subset profile that is comparable to that reported for human monocytes (Galiegue et al. 1995; Whyte et al. 2009). Thus, U937 cells served as relevant models to assess the effect of select cannabinoids on HIV-1 Tat-enhanced adhesion to ECM proteins.

Initial experiments demonstrated that U937 cells adhered in a Tat dose-related fashion to proteins of the ECM. Statistically-significant adhesion to Coll IV, LM and ECM gel was obtained when Tat was employed at a concentration of 10 nM, but maximal adhesion was obtained when this HIV gene product was used at a concentration of 50 nM. While a 50 nM concentration is relatively high, it is not unreasonable in the context of the microenvironment of a Tat-secreting, HIV competently-infected cell. Furthermore, in the present study, Tat was used in a dose-response mode in order to obtain "proof-of-principle" for its specificity of action. In addition, a higher level of adhesion at the 50 nM concentration of Tat was obtained for Coll IV or LM as compared with ECM gel. A possible explanation for this outcome is that ECM gel is a complex mixture that upon polymerization forms a reconstituted basement membrane consisting of Coll IV, LM, heparan sulfate proteoglycan, entactin, and other minor components. Thus, the time kinetics used in the present study may not have been optimal for adhesion when using ECM gel as a matrix substrate. Nevertheless, the results of the present study indicate that U937 cells exhibit Tat-enhanced adherence to all three ECM substrates.

Treatment of U937 cells with CP55,940 resulted in inhibition of Tat-enhanced adhesion to all three ECM substrates. Scanning electron microscopy confirmed the pharmacological results and provided insight regarding the interaction of U937 cells with Coll IV. Cells not exposed to Tat exhibited a rounded conformation while those treated with Tat appeared flattened, and spread-out and exhibited numerous thin, finger-like projections that extended to the ECM substrate. In contrast, U937 cells treated with Tat in the presence of CP55,940

were rounded in appearance and displayed fewer finger-like projections. In these experiments, CP55,940 was used at a concentration of 1 μM, a concentration that when used in the absence of Tat exerted no overt morphological changes on U937 cells. Thus, at the morphological level, U937 cells exposed to Tat in the presence of CP55,940 exhibited fewer apparent anchorage points to the ECM substrate. These results suggest that select cannabinoids either affect cytoskeletal rearrangement on U937 cells or inhibit the expression of adhesion molecules by these cells that are critical to the extracellular matrix adherence process. Results obtained using confocal microscopy were consistent with those derived through the use of scanning electron microscopy and, in addition, revealed that the distribution of actin appeared prominent at projections of cells treated with Tat. Furthermore, β_1 integrins appeared to colocalize at these extensions. On the other hand, cells exposed to Tat and treated with THC or CP55,940 exhibited a distributional pattern of actin and β_1 integrins that approximated that of cells not treated with Tat. Consistent with these observations, it has been reported that THC can disrupt microtubules and microfilaments in PC12 cells derived from a pheochromocytoma of the rat adrenal medulla (Tahir et al. 1992). It also has been reported that, upon stimulation of the CB2R, human neutrophil-like HL60 cells rapidly extend and retract one or more pseudopods containing F-actin in different directions instead of developing front/rear polarity typically exhibited by migrating leukocytes (Kuhihara et al. 2006). These reports, taken in context that it has been indicated that cellular adhesion to Coll IV and LM can be mediated through heterodimeric receptors containing β_1 integrins (Rosales and Juliano 1995), suggest that THC and CP55,940 alter cytoskeletal rearrangement that is requisite for adhesion of Tat-stimulated U937 cells to targets on ECM components such as L-Arginyl-Glycyl-L-Aspartic acid (RGD) motifs that serve as interactive points. In this fashion, by inhibiting the interaction of U937 finger-like projections with RGD motifs, THC and CP55,940 could dampen the induction of signal transductional activities that lead to activation of macrophage-like cell pathways that contribute to enhanced cell-endothelium and cell-ECM interactions involved in cellular transmigration of the BBB.

In order to assess for a pharmacological linkage to a cannabinoid receptor in cannabinoid-mediated inhibition of Tat-enhanced adhesion of U937 cells to ECM substrates, a select number of cannabinoid agonists and antagonists was used in experiments. Treatment of cells with Tat in concert with the partial agonist THC or with the full agonist CP55,940 resulted in inhibition of Tat-enhanced adhesion to ECM components. Similar inhibitory results were obtained when U937 cells were treated with Tat in the presence of the CB2R-selective ligand O-2137. In contrast, the CB1R-selective ligand ACEA had no effect on Tat-enhanced adhesion to ECM proteins, a result that was consistent with the observation that the CB1R was not detected in these cells by RT-PCR or Western immunoblotting. Additional experiments, performed using cannabinoid receptor-selective antagonists, demonstrated that the CB2R-selective antagonist SR2 reversed inhibition mediated by CP55,940 while the CB1R-selective antagonist SR1 did not. Thus, the collective pharmacological data converged on an outcome indicative of a functional linkage of the CB2R to cannabinoid-mediated inhibition of Tat-enhanced adhesion of U937 cells to the ECM.

The present investigation also revealed that U937 cells express GPR55 and that Abn-CBD, a putative agonist of GPR55 (Johns et al. 2007), inhibited U937 cell adhesion. This G protein-

coupled receptor has been identified *in silico* as a putative cannabinoid receptor (Baker et al. 2006) and it has been suggested that lysophosphatidylinositol and its 2-arachidonoyl derivative are its endogenous ligands (Oka et al. 2007; Oka et al. 2009). It has been proposed that GPR55 is functionally relevant in cannabinoid-mediated action due to crosstalk with the CB2R. Thus, the interplay of these receptors could be involved in optimizing select immune responses such as alleviation of excessive tissue injury (Irving 2011). Balenga et al. (2011) has reported that simultaneous activation of GPR55 and the CB2R enhances signaling pathways involving Rho GTPases, Rho A, and cdc42, in addition to increasing RhoA-mediated neutrophil chemotaxis. Nevertheless, the role of GPR55 in cannabinoid-mediated effects on Tat-enhanced adhesion to ECM proteins remains unresolved and a more extensive analysis is required to delineate its functional relevance in this process.

Finally, the present set of experiments on the effect of cannabinoids on Tat-enhanced adhesion to ECM substrates was performed using a two-dimensional extracellular matrix substrate and the question remains as to whether cannabinoid-mediated effects on such a construct were translatable to a three-dimensional matrix. To address for this potential confound, ECM gel was used as the matrix construct in cell migration chambers. ECM gel was employed since it represented the most complex substratum used and LM and Coll IV were inclusive protein components. Cells treated with vehicle exhibited a minimal level of migration through the ECM gel composite, cells treated with Tat exhibited a three-fold increase in the level of migration through the ECM gel composite, and cells exposed to Tat in the context of exposure to CP55,940 exhibited inhibition of migration through the ECM gel composite. The level of inhibition of migration through the ECM gel composite was comparable to that recorded for vehicle-treated cells. These results are consistent with the conclusion that the matrices used in the present study did not simply serve as physical barriers to the passage of U937 cells.

Conclusions

The Tat protein of the HIV promoted adhesion of human U937 cells to ECM proteins. This enhancement in adhesion was inhibited by cannabinoids that activate the CB2R. The cannabinoid-mediated inhibition in adhesion was associated with U937 cell morphological changes as determined by scanning electron microscopy. Cells exposed to Tat exhibited numerous thin, finger-like projections that extended to the ECM substrate while those exposed to Tat in the presence of cannabinoid displayed a minimal number of finger-like projections extending to the matrix substrate. Since the attachment process serves as an environmental cue that sets into motion a cascade of intracellular events that result in cytoskeletal reorientation, differential gene expression, and promotion of cell transmigration (Berrier and Yamada 2007), these results suggest that the CB2R has potential to serve as a molecular target for ablating monocyte transmigration of the BBB in response to HIV infection.

Acknowledgments

References

1. Rubin LL, Staddon JM. The cell biology of the blood brain barrier. Annu Rev Neurosci. 1999; 22:11–28.10.1146/annurev.neuro.22.1.11 [PubMed: 10202530]

2. Lukashev ME, Werb Z. ECM signaling: orchestrating cell behaviour and misbehaviour. Trends Cell Biol. 1998; 8:437–41.10.1016/S0962-8924(98)01362-2 [PubMed: 9854310]

3. Mareel M, Leroy A. Clinical, cellular and molecular aspects of cancer invasion. Physiol Rev. 2003; 83:337–76.10.1152/physrev.00024.2002 [PubMed: 12663862]

4. Larsen M, Artym VV, Green JA, Yamada KM. The matrix reorganized: extracellular matrix remodeling and integrin signaling. Curr Opin Cell Biol. 2006; 18:463–71.10.1016/j.ceb. 2006.08.009 [PubMed: 16919434]

5. Berrier AL, Yamada KM. Cell-matrix adhesion. J Cell Physiol. 2007; 213:565–73.10.1002/jcp. 21237 [PubMed: 17680633]

6. Buckner CM, Luers AJ, Calderon TM, Eugenin EA, Berman JW. Neuroimmunity and the blood-brain barrier: molecular regulation of leukocyte transmigration and viral entry into the nervous system with a focus on neuroAIDS. J Neuroimmune Pharmacol. 2006; 1:160–81.10.1007/ s11481-006-9017-3 [PubMed: 18040782]

7. Schneider J, Kaaden O, Copeland TD, Oroszlan S, Hunsmann G. Shedding and interspecies type sero-reactivity of the envelope glycoprotein gp120 of the human immunodeficiency virus. J Gen Virol. 1986; 67:2533–8.10.1099/0022-1317-67-11-2533 [PubMed: 2431105]

8. Ensoli B, Buonaguro L, Barillari G, Fiorelli V, Gendelman R, Morgan RA, et al. Release, uptake, and effects of extracellular human immunodeficiency virus type 1 Tat protein on cell growth and viral transactivation. J Virol. 1993; 67:277–87. [PubMed: 8416373]

9. Zink WE, Zheng J, Persidsky Y, Poluektova L, Gendelman HE. The neuropathogenesis of HIV-1 infection. FEMS Immunol Med Microbiol. 1999; 26:233–41.10.1111/j.1574-695X.1999.tb01394.x [PubMed: 10575134]

10. Glass JD, Wesselingh SL, Selnes OA, McArthur JC. Clinical-neuropathologic correlation in HIV-associated dementia. Neurology. 1993; 43:2230–7.10.1212/WNL.43.11.2230 [PubMed: 8232935]

11. Laspia MF, Rice AP, Matthews MB. HIV-1 Tat protein increases transcriptional initiation and stabilizes elongation. Cell. 1989; 59:283–92.10.1016/0092-8674(89)90290-0 [PubMed: 2553266]

12. Lafrenie RM, Wahl LM, Epstein JS, Hewlett IK, Yamada KM, Dhawan S. HIV-1-Tat modulates the function of monocytes and alters their interactions with microvessel endothelial cells. J Immunol. 1996; 156:1638–45. [PubMed: 8568270]

13. Chang HK, Gallo RC, Ensoli B. Regulation of cellular gene expression and functions by the human immunodeficiency virus type 1 Tat protein. J Biomed Sci. 1995; 2:189–202. [PubMed: 11725056]

14. Pu H, Tian J, Flora G, Lee YW, Nath A, Hennig B, et al. HIV-1 Tat protein upregulates inflammatory mediators and induces monocyte invasion into the brain. Mol Cell Neurosci. 2003; 24:224–37.10.1016/S1044-7431(03)00171-4 [PubMed: 14550782]

15. D'Aversa TG, Yu KO, Berman JW. Expression of chemokines by human fetal microglia after treatment with the human immunodeficiency virus type 1 protein Tat. J Neurovirol. 2004; 10:86–97.10.1080/13550280490279807 [PubMed: 15204927]

16. de Paulis A, De Palma R, Di Gioia L, Carfora M, Prevete N, Tosi G, et al. Tat protein is an HIV-1-encoded β-chemokine homolog that promotes migration and up-regulates CCR3 expression on human FcγRI+ cells. J Immunol. 2000; 165:7171–9. [PubMed: 11120849]

17. Avraham HK, Jiang S, Lee TH, Prakash O, Avraham S. HIV-1 Tat-mediated effects on focal adhesion assembly and permeability in brain microvascular endothelial cells. J Immunol. 2004; 173:6228–33. [PubMed: 15528360]

18. Eugenin EA, Dyer G, Calderon TM, Berman JW. HIV-1 tat protein induces a migratory phenotype in human fetal microglia by a CCL2 (MCP-1)-dependent mechanism: possible role in NeuroAIDS. Glia. 2005; 49:501–10.10.1002/glia.20137 [PubMed: 15578658]

19. Cabral GA, Staab A. Effects on the immune system. Handb Exp Pharmacol. 2005; 168:385–423. [PubMed: 16596782]

20. Raborn ES, Cabral GA. Cannabinoid inhibition of macrophage migration to the trans-activating (Tat) protein of HIV-1 is linked to the CB2 cannabinoid receptor. J Pharmacol Exp Ther. 2010; 333:319–27.10.1124/jpet.109.163055 [PubMed: 20089805]

21. Kong W, Li H, Tuma RF, Ganea D. Selective CB2 receptor activation ameliorates EAE by reducing Th17 differentiation and immune cell accumulation in the CNS. Cell Immunol. 2014; 287:1–17.10.1016/j.cellimm.2013.11.002 [PubMed: 24342422]

22. Bradford MM. A rapid and sensitive method for the quantitation of microgram quantities of protein utilizing the principle of protein-dye binding. Anal Biochem. 1976; 72:248–54.10.1016/0003-2697(76)90527-3 [PubMed: 942051]

23. Nowell KW, Petit DA, Cabral WA, Zimmerman HW Jr, Abood ME, Cabral GA. High level expression of the human CB2 cannabinoid receptor using a baculovirus system. Biochem Pharmacol. 1998; 55:1893–1905.10.1016/S0006-2952(98)00081-1 [PubMed: 9714308]

24. Arya SK, Guo C, Josephs SF, Wong-Staal F. Trans-activator gene of human T-lymphotropic virus type III (HTLV-III). Science. 1985; 229:69–73.10.1126/science.2990040 [PubMed: 2990040]

25. Dayton AI, Sodroski JG, Rosen CA, Goh WC, Haseltine WA. The trans-activator gene of the human T-lymphotropic virus type III is required for replication. Cell. 1986; 44:941–7.10.1016/0092-8674(86)90017-6 [PubMed: 2420471]

26. Watson K, Edwards RJ. HIV-1-trans-activating (Tat) protein: both a target and a tool in therapeutic approaches. Biochem Pharmacol. 1999; 58:1521–8.10.1016/S0006-2952(99)00209-9 [PubMed: 10535742]

27. Albini A, Ferrini S, Benelli R, Sforzini S, Giunciuglio D, Aluigi MG, et al. HIV-1 Tat protein mimicry of chemokines. Proc Natl Acad Sci USA. 1998; 95:13153–8.10.1073/pnas.95.22.13153 [PubMed: 9789057]

28. Fraga D, Raborn ES, Ferreira GA, Cabral GA. Cannabinoids inhibit migration of microglial-like cells to the HIV protein Tat. J Neuroimmune Pharmacol. 2011; 6:566–77.10.1007/s11481-011-9291-6 [PubMed: 21735070]

29. Ghezzi S, Noonan DM, Aluigi MG, Vallanti G, Cota M, Benelli R, et al. Inhibition of CXCR4-dependent HIV-1 infection by extracellular HIV-1 Tat. Biochem Biophys Res Commun. 2000; 270:992–6.10.1006/bbrc.2000.2523 [PubMed: 10772939]

30. Dhawan S, Vargo M, Meltzer MS. Interactions between HIV-infected monocytes and the extracellular matrix: increased capacity of HIV-infected monocytes to adhere to and spread on extracellular matrix associated with changes in extent of virus replication and cytopathic effects in infected cells. J Leukoc Biol. 1992; 52:62–9. [PubMed: 1640176]

31. Song HY, Ryu J, Ju SM, Park LJ, Lee JA, Choi SY, et al. Extracellular HIV-1 Tat enhances monocyte adhesion by up-regulation of ICAM-1 and VCAM-1 gene expression via ROS-dependent NFκB activation in astrocytes. Exp Mol Med. 2007; 39:27–37.10.1038/emm.2007.4 [PubMed: 17334226]

32. Weiss JM, Nath A, Major EO, Berman JW. HIV-1Tat induces monocyte chemoattractant protein-1-mediated monocyte transmigration across a model of the human blood-brain barrier and up-regulates CCR5 expression on human monocytes. J Immunol. 1999; 163:2953–9. [PubMed: 10453044]

33. Baeten KM, Akassoglou K. Extracellular matrix and matrix receptors in blood-brain barrier formation and stroke. Dev Neurobiol. 2011; 71:1018–39.10.1002/dneu.20954 [PubMed: 21780303]

34. Muller WA, Randolph GJ. Migration of leukocytes across endothelium and beyond: molecules involved in the transmigration and fate of monocytes. J Leukoc Biol. 1999; 66:689–704. [PubMed: 10534127]

35. Mitola S, Sozzani S, Luini W, Primo L, Borsatti A, Weich H, et al. Tat-human immunodeficiency virus-1 induces human monocyte chemotaxis by activation of vascular endothelial growth factor receptor-1. Blood. 1997; 90:1365–72. [PubMed: 9269752]

36. Sundstrom C, Nilsson K. Establishment and characterization of a human histiocytic lymphoma cell line (U-937). Int J Cancer. 1976; 17:565–77.10.1002/ijc.2910170504 [PubMed: 178611]

37. Pucillo CE, Colombatti A, Vitale M, Salzano S, Rossi G, Formisano S. Interactions of promonocytic U937 cells with proteins of the extracellular matrix. Immunology. 1993; 80:248–52. [PubMed: 8262552]

38. Zella D, Barabitskaja O, Burns JM, Romerio F, Dunn DE, Revello MG, et al. Interferon-gamma increases expression of chemokine receptors CCR1, CCR3, and CCR5, but not CXCR4 in monocytoid U937 cells. Blood. 1998; 91:4444–50. [PubMed: 9616137]

39. Cassol E, Alfano M, Biswas P, Poli G. Monocyte-derived macrophages and myeloid cell lines as targets of HIV-1 replication and persistence. J Leukoc Biol. 2006; 80:1018–30.10.1189/jlb. 0306150 [PubMed: 16946020]

40. Emiliani S, Fischle W, Ott M, Van Lint C, Amella CA, Verdin E. Mutations in the tat gene are responsible for human immunodeficiency virus type 1 postintegration latency in the U1 cell line. J Virol. 1998; 72:1666–70. [PubMed: 9445075]

41. Leghmari K, Contreras X, Moureau C, Bahraoui E. HIV-1 Tat protein induces TNF-α and IL-10 production by human macrophages: differential implication of PKC-βII and -δ isozymes and MAP kinases ERK1/2 and p38. Cell Immunol. 2008; 254:46–55.10.1016/j.cellimm.2008.06.011 [PubMed: 18692180]

42. Galiegue S, Mary S, Marchand J, Dussossoy D, Carriere D, Carayon P, et al. Expression of central and peripheral cannabinoid receptors in human immune tissues and leukocyte subpopulations. Eur J Biochem. 1995; 232:54–61.10.1111/j.1432-1033.1995.tb20780.x [PubMed: 7556170]

43. Whyte LS, Ryberg E, Sims NA, Ridge SA, Mackie K, Greasley PJ, et al. The putative cannabinoid receptor GPR55 affects osteoclast function in vitro and bone mass in vivo. Proc Natl Acad Sci USA. 2009; 106:16511–6.10.1073/pnas.0902743106 [PubMed: 19805329]

44. Tahir SK, Trogadis JE, Stevens JK, Zimmerman AM. Cytoskeletal organization folllowing cannabinoid treatment in undifferentiated and differentiated PC12 cells. Biochem Cell Biol. 1992; 70:1159–1173.10.1139/o92-162 [PubMed: 1297339]

45. Kurihara R, Tohyama Y, Matsusaka S, Naruse H, Kinoshita E, Tsujioka T, Katsumata Y, Yamamura H. Effects of peripheral cannabinoid receptor ligands on motility and polarization in neutrophil-like HL60 cells and human neutrophils. J Biol Chem. 2006; 281:12908–12918.10.1074/jbc.M510871200 [PubMed: 16513651]

46. Rosales C, Juliano RL. Signal transduction by cell adhesion receptors in leukocytes. J Leuk Biol. 1995; 57:189–198.

47. Johns DG, Behm DJ, Walker DJ, Ao Z, Shapland EM, Daniels DA, et al. The novel endocannabinoid receptor GPR55 is activated by atypical cannabinoids but does not mediate their vasodilator effects. Br J Pharmacol. 2007; 152:825–31.10.1038/sj.bjp.0707419 [PubMed: 17704827]

48. Baker D, Pryce G, Davies WL, Hiley CR. In silico patent searching reveals a new cannabinoid receptor. Trends Pharmacol Sci. 2006; 27:1–4.10.1016/j.tips.2005.11.003 [PubMed: 16318877]

49. Oka S, Nakajima K, Yamashita A, Kishimoto S, Sugiura T. Identification of GPR55 as a lysophosphatidylinositol receptor. Biochem Biophys Res Commun. 2007; 362:928–34.10.1016/j.bbrc.2007.08.078 [PubMed: 17765871]

50. Oka S, Toshida T, Maruyama K, Nakajima K, Yamashita A, Sugiura T. 2-Arachidonoyl-sn-glycero-3-phosphoinositol: a possible natural ligand for GPR55. J Biochem. 2009; 145:13–20.10.1093/jb/mvn136 [PubMed: 18845565]

51. Irving A. New blood brothers: the GPR55 and CB2 partnership. Cell Res. 2011; 21:1391–2.10.1038/cr.2011.77 [PubMed: 21537344]

52. Balenga NA, Aflaki E, Kargl J, Platzer W, Schroder R, Blattermann S, et al. GPR55 regulates cannabinoid 2 receptor-mediated responses in human neutrophils. Cell Res. 2011; 21:1452–69.10.1038/cr.2011.60 [PubMed: 21467997]
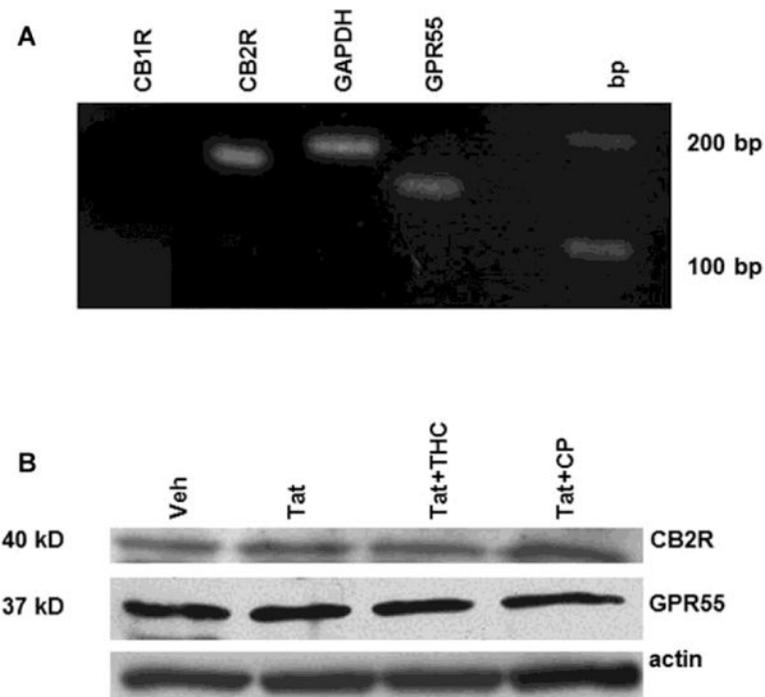
Fig. 1.
U937 human monocyte-like cells express the CB2R and GPR55. (A) Real-time SYBR green RT-PCR demonstrated the presence of mRNA for the CB2R (185 bp amplicon) and GPR55 (137 bp amplicon), but not for the CB1R. Constitutively expressed GAPDH mRNA amplification product was used as a positive internal control. (B) Western immunoblotting demonstrated the presence of protein for the CB2R and GPR55. Actin was used as a control to verify comparable loading of samples.
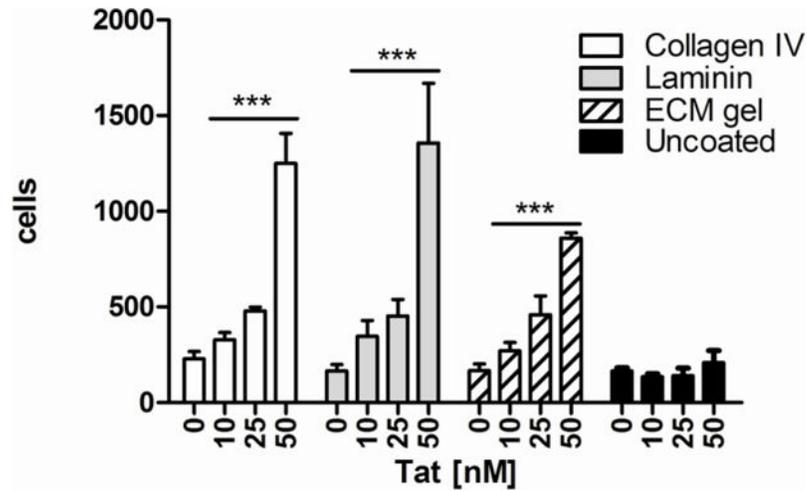
Fig. 2.
Tat stimulates adhesion of U937 monocyte-like cells to ECM proteins. Adhesion of U937 cells to uncoated tissue culture wells or to wells coated with Coll IV, LM, and ECM gel was assessed following treatment (2h) with Tat (10, 25, or 50 nM). Results are presented as the mean ± SD of a representative experiment. ***p<0.001, Cells treated with Tat compared with cells not treated with Tat.
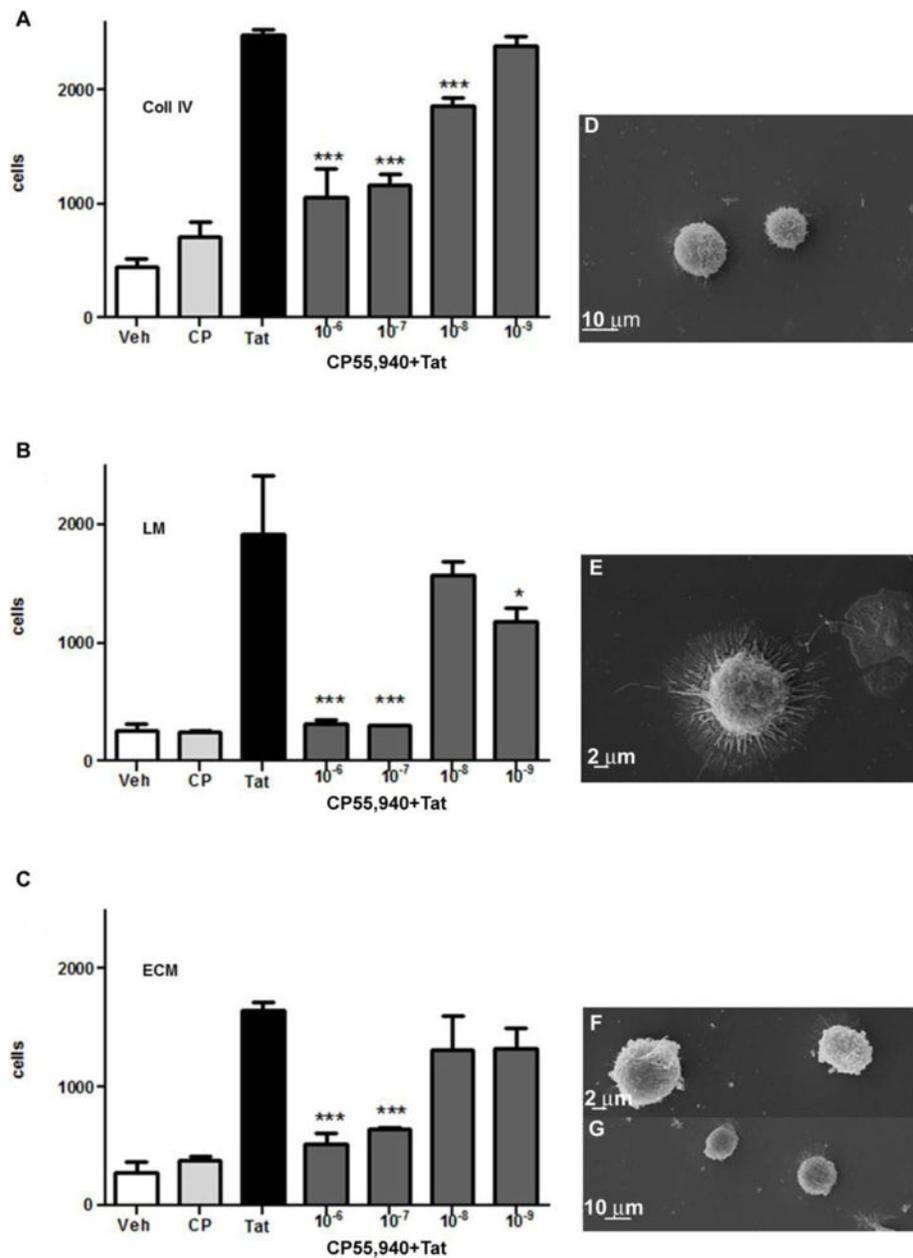
Fig. 3.
CP55,940 inhibits Tat-enhanced U937 cell adhesion to extracellular matrix proteins: (A–C). U937 cells were treated (2h) with Tat (50 nM) in the presence or absence of the CB1R/CB2R full agonist, CP55,940 (1 nM– 1 μM) and adhesion to Coll IV (A), LM (B), or ECM gel (C) was assessed. Results are presented as mean ± SD of one representative experiment performed in triplicate. *p<0.05, ***p<0.001: Tat + CP55,940 vs. Tat + Vehicle. (D–G). Scanning electron micrographs of U937 cells seeded on Coll IV demonstrating morphological alterations in adherence following treatment with Veh (D), Tat (50 nM) + Veh (E), Tat (50 nM) + 1 μM THC (F), or Tat + 1 μM CP55,940 (G). CP=CP55,940.
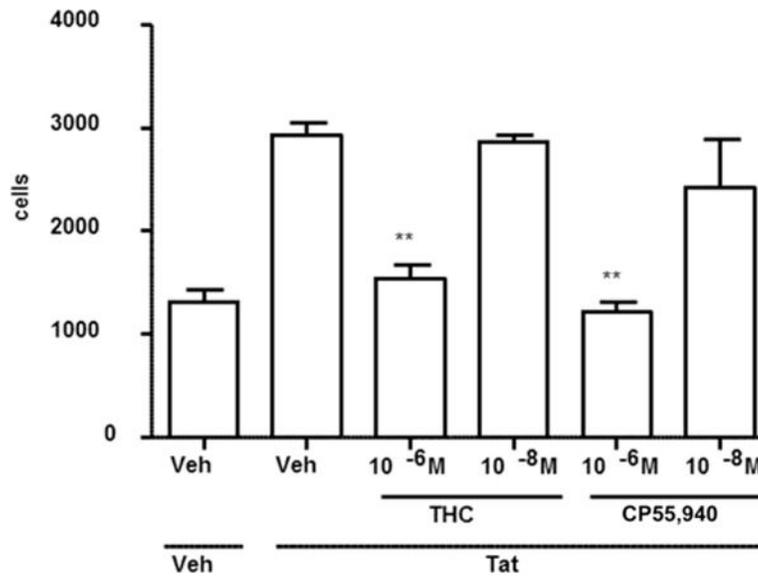
Fig. 4.
The cannabinoids THC and CP55,940 inhibit HIV-1 Tat-mediated passage of U937 monocyte-like cells through ECM gel. Results are presented as the mean ± SD of a representative experiment. **$p<0.01$, Tat (50 nM) + cannabinoid-treated cells compared with Tat (50 nM) + vehicle-treated cells.
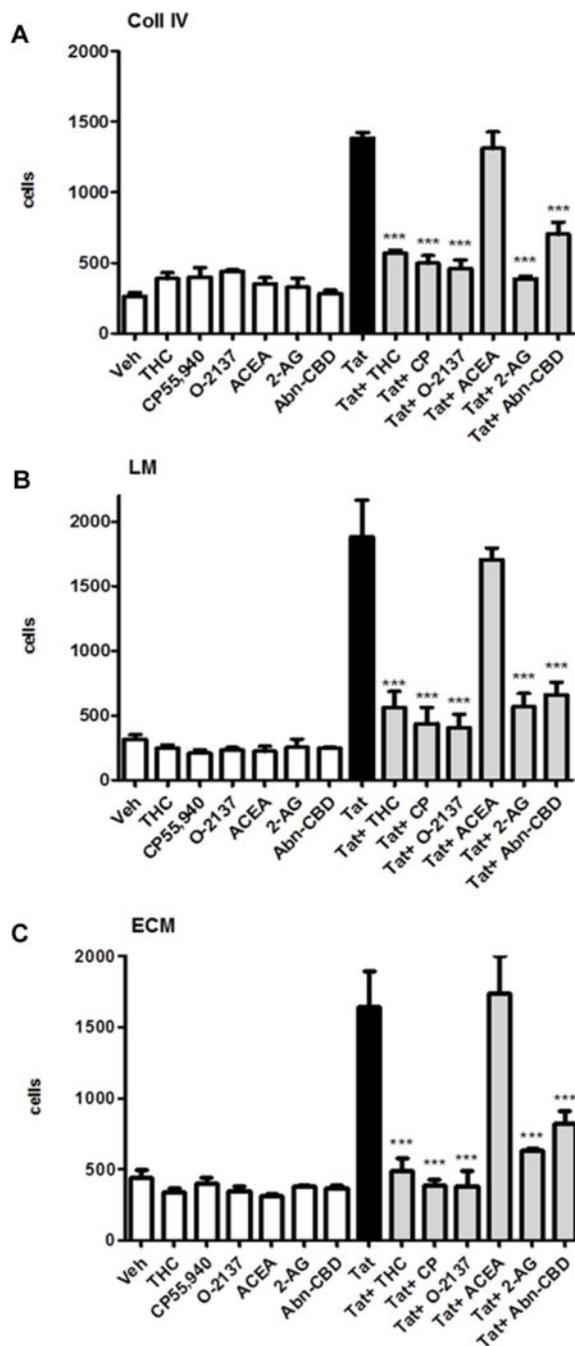
Fig. 5.
Cannabinoid effect on U937 cell adhesion to extracellular matrix proteins: Coll IV (A), LM (B), ECM gel (C). U937 cells were treated (2h) with Tat (50 nM) in the presence or absence of cannabinoids (1 µM) and adhesion to ECM substrates was assessed (30 min). Results are presented as mean ± SD of one representative experiment. *** p<0.001 Tat+ cannabinoid vs. Tat + vehicle.
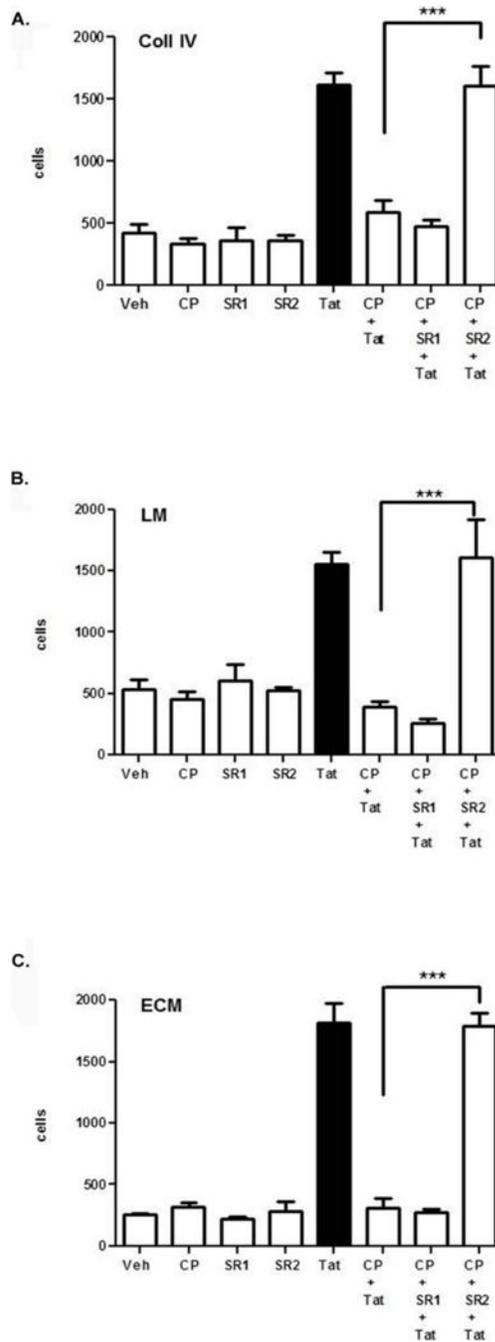
Fig. 6.
Treatment of U937 cells with the CB2R-selective antagonist SR144528 (SR2) reverses CP55,940-mediated inhibition of Tat-enhanced cellular adhesion to ECM proteins. U937 cells were treated with antagonist (1μM, 30 min) before being treated (2h) with CP55,940 (1 μM)+Tat (50 nM) and adhesion to ECM components was assessed: Coll IV (A); LM (B), ECM gel (C). Results are presented as mean ± SD of one representative experiment. *** p<0.001. CP=CP55,940.
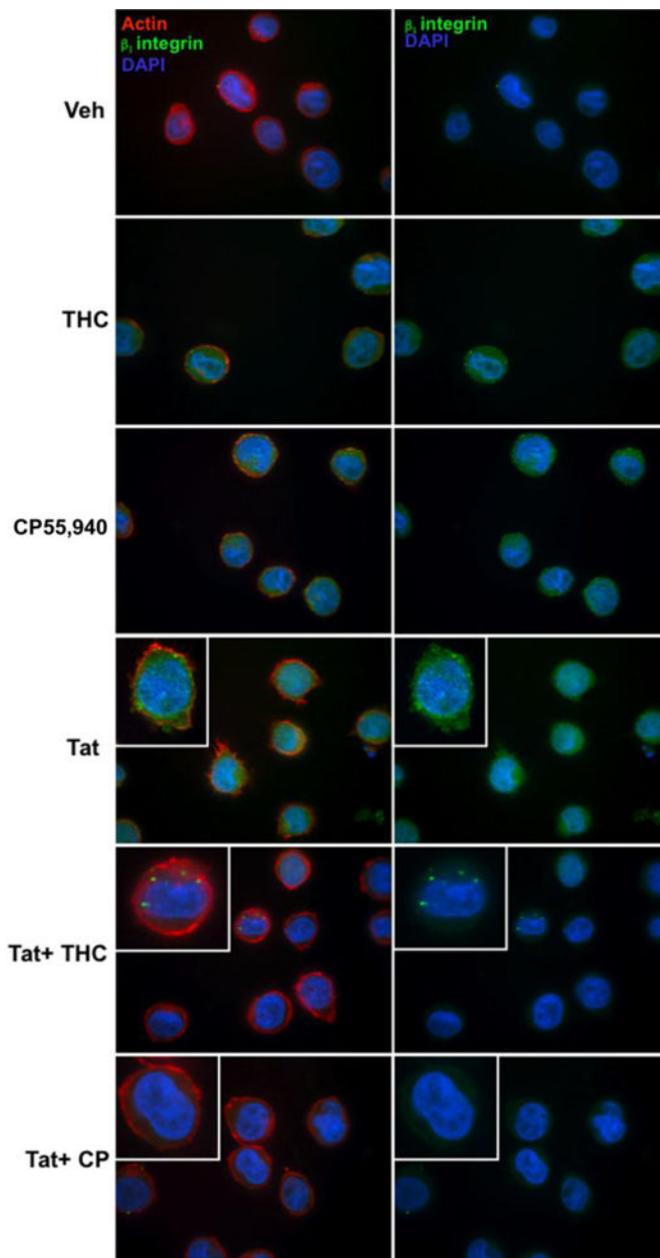
Fig. 7.
Treatment with THC or CP55,940 alters distribution of β_1-integrin and polymerized actin. U937 cells were treated (2h) with cannabinoid (THC or CP55,940)(1μM) plus Tat (50 nM), then seeded on Coll IV-coated chamber slides and allowed to adhere (1h). Fixed cells were stained with anti-human-β_1-integrin-FITC antibody followed by Phalloidin-AlexaFluor594 to visualize F-actin. Cell nuclei were counterstained with DAPI. The left column depicts the merged images for actin and β_1- integrin while the right column depicts images for β_1-integrin. Insets depict magnified (200x) singular cells. Images-100x.